Appl Phys B (2010) 99: 441–447
DOI 10.1007/s00340-010-3900-6

Applied Physics B
Lasers and Optics

Ultrahigh-repetition-rate bound-soliton fiber laser

L.M. Zhao · D.Y. Tang · D. Liu

Received: 18 September 2009 / Revised version: 20 November 2009 / Published online: 5 February 2010

Abstract Ultrahigh-repetition-rate (over 100 GHz) bound-soliton pulses were experimentally generated in a fiber laser. Through incorporating a Loyt-type filter made of a piece of high birefringent fiber and an intracavity polarizer in a fiber laser, we found that not only ultrahigh-repetition-rate single-pulse soliton but also bound-soliton trains could be generated. Numerical simulations confirm the experimental observations.

1 Introduction

High-repetition-rate pulse lasers play a key role in ultrahigh speed optical communication systems. Recently, several authors reported generation of optical pulses with over 100 GHz repetition rates directly from fiber lasers based on the self-induced modulation instability oscillation (MIO) technique [1–4]. Franco et al. were the first who experimentally observed MIO in a fiber laser [1]. In an experiment with a fiber laser passively mode locked with the nonlinear polarization rotation (NPR) technique, they found that a high-repetition-rate cw soliton pulse train could be automatically generated in the laser even without a polarizer inserted in the cavity. They proved experimentally that the observed high-repetition-rate pulse train was generated due to the MIO. The self-induced MIO technique was later used by de Matos et al. to generate a cw soliton pulse train with 262 GHz repetition rate using highly nonlinear dispersion-shifted fibers to construct the laser cavity [2]. Yoshida and Nakazawa reported a more stable version of the self-induced MIO fiber laser [3]. It was shown that through inserting an intracavity Fabry-Pérot filter with a free spectral range equal to the modulation instability (MI) gain peak, low threshold MIO could be induced. In addition, the narrow band optical filter could further suppress the super-mode noise of the laser and stabilize the pulse train.

MI is a well-known process occurring in nonlinear dispersive media due to the interplay between the nonlinearity and anomalous dispersion [5, 6]. Anomalous dispersion is essential for the appearance of MI. Very recently Sylvestre et al. have demonstrated that high-repetition-rate pulses could also be generated in fiber lasers with a normal dispersion cavity [7]. The result suggests that apart from the MIO, other processes could also be used to generate high-repetition-rate pulses in a fiber laser. In fact, Quiroga et al. had proposed a so-called dissipative four-wave-mixing (DFWM) passive mode-locking technique [8]. It was shown numerically that a cw pulse train with well-defined repetition rate could automatically build up in a fiber laser with a frequency-dependent gain profile that has two symmetric peaks. Determined by the gain profile laser oscillations at the two gain peak wavelengths are initially excited. Energy of the oscillations is then transferred to the other wavelengths through the four-wave-mixing process. However, due to that these wavelengths are outside of the laser gain bandwidth, no oscillations can build up and the energy is dissipated. As a result of such a DFWM process a stable unchirped pulse train with a well-defined repetition rate is then generated. The mode locking works in either normal or anomalous dispersion cavity fiber lasers. Ultrahigh-repetition-rate mode-locked pulses could be generated with the mode-locking technique through appropriately selecting the laser parame-

L.M. Zhao · D.Y. Tang (✉)
School of Electrical and Electronic Engineering, Nanyang Technological University, Singapore, 639798, Singapore
e-mail: edytang@ntu.edu.sg
Fax: +65-6792-0415

D. Liu
Faculty of Physics and Electronics, Hubei University, Wuhan, China

ters [9]. Indeed, Sylvestre et al. have also identified that the high-repetition-rate pulse generation in their laser is due to the DFWM process [8].

So far all researches on the high-repetition-rate pulse fiber lasers have focused on the single-pulse train, namely the repeating unit of the laser emission is a single peak soliton. It is well known that a fiber laser can also emit multi-pulse solitons, which are another form of solitary waves formed in fiber lasers [10, 11]. Extensive experimental studies have shown that the multi-pulse solitons have exactly the same properties as those of the single-pulse solitons, such as energy quantization [12, 13], harmonic mode locking [14–17] and period-doubling bifurcations [18, 19]. Therefore, it would be interesting to know whether high-repetition-rate multi-pulse solitons could also be generated in a fiber laser.

In this paper, we report on a novel high-repetition-rate fiber laser that can emit not only single-pulse soliton train but also bound-soliton pulse train. We show experimentally that by inserting a segment of high birefringence (HiBi) fiber together with an intracavity polarizer in a fiber ring laser, passive DFWM mode locking can self-start in the laser. Consequently, a high-repetition-rate mode-locked pulse train with a repetition rate of 111 GHz is generated. Apart from the high-repetition single soliton pulse train, under strong pumping a high-repetition-rate bound-soliton pulse train with the same repetition rate is also firstly obtained. Formation of the high-repetition-rate single-pulse soliton or the bound-soliton train in our laser was further numerically simulated. It shows that formation of the bound-soliton pulse train is a natural development of the single-pulse soliton train under stronger pumping.

2 Experimental setup and results

Our fiber laser is schematically shown in Fig. 1. It has a typical cavity configuration as that used for the fiber lasers passively mode locked with the NPR technique [10]. A 17.6-meter-long erbium-doped fiber (EDF-1480-T6) was used as the gain medium. The output coupler and the wavelength division multiplexer are both made of standard single mode fiber (SMF). A polarization-independent isolator is inserted in the cavity to force the unidirectional operation of the ring and suppress the build-up of the stimulated Brillouin scattering. Two polarization controllers, one consisting of two quarter-wave plates and the other two quarter-wave plates and one half-wave plate, are used to adjust the polarization of the light. A segment of HiBi fiber is inserted between the output coupler and the erbium-doped fiber. The polarization controllers, polarization-independent isolator, and the polarizer are mounted on a 7-cm-long fiber bench.

It is well known that due to the existence of a polarizer in the cavity, there is intrinsically a Lyot type of filter effect in

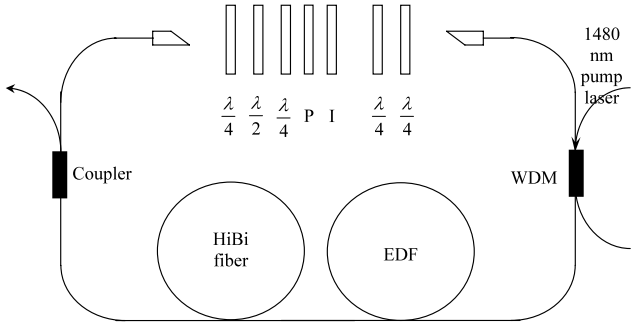

Fig. 1 Schematic of the experiment setup. EDF: erbium-doped fiber; WDM: wavelength division multiplexer; I: isolator; P: polarizer

the fiber laser shown in Fig. 1 [10]. We note that inserting a segment of HiBi fiber in the laser cavity has the consequence that the spectral bandwidth of the Lyot filter transmission lines is significantly reduced. The free spectral range (FSR) of the Lyot filter is determined by the birefringence of the cavity. In the case that the other cavity fibers used are only the weakly birefringence fibers, one can roughly consider that the cavity birefringence is contributed by the HiBi fiber inserted. Therefore, the FSR of the filter is mainly determined by the birefringence of the HiBi fiber and is calculated as

$$\Delta\lambda = \frac{\lambda^2}{BL} \tag{1}$$

where $\Delta\lambda$ is the free spectral range, λ is the central wavelength of the light propagating in the fiber, B is the fiber birefringence coefficient, and L is the length of the HiBi fiber.

In an anomalous dispersion cavity fiber laser MI always exists. For our fiber laser without the HiBi fiber in the cavity, under normal laser operation the MI wavelength shift is found to be about 1 nm, which corresponds to ∼125 GHz if the central wavelength of the laser emission is assumed to be 1550 nm. To take advantage of the MI for stable high-repetition-rate pulse generation, we have selected the FSR of the Lyot filter to possibly match the MI gain peak. As the birefringence coefficient of our HiBi fiber is 2.2×10^{-4}, we have chosen the HiBi fiber length to be 11.5 m.

Figure 2 shows the experimental results obtained. Due to the spectral filtering effect of the Lyot filter and the laser gain bandwidth limiting, mode locking of the laser through the DFWM process self-starts. Figure 2(a) shows a typical mode-locked pulse train obtained at a relatively weak pump power, and Fig. 2(c) is the corresponding optical spectrum. The pulse separation measured is 8.98 ps, which corresponds to the spectral peak separation of the measured optical spectrum shown in Fig. 2(c), indicating that the mode-locked pulse repetition rate is determined by the frequency-spacing of the transmission peaks of the Lyot filter. The measured optical spectrum has a symmetric spectral intensity

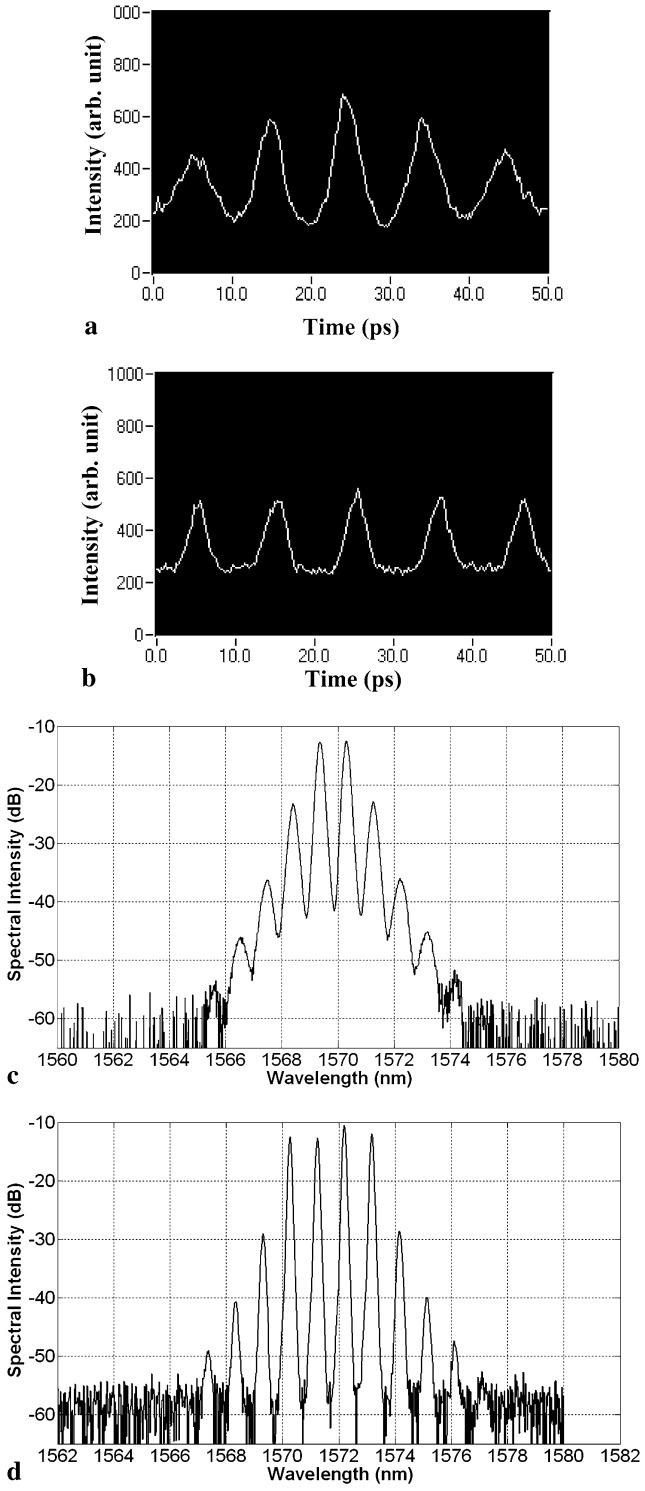

Fig. 2 Autocorrelation traces (**a**, **b**) and optical spectra (**c**, **d**) of the high-repetition-rate single-pulse emission of the fiber laser. From (**a**) to (**b**) the pump power of the laser was increased

distribution, which is a characteristic of the DFWM mode locking [8]. We note that even under the DFWM mode locking, the mode-locked pulse train shows a small but obvious pulse intensity modulation. We attribute the pulse intensity modulation as a result of the MI of the two main spectral components. As the MI frequency is now smaller than the FSR of the Lyot filter, it causes the pulse intensity variation and broadening of the spectral lines shown in Fig. 2(c). The MI frequency is proportional to the square root of the average power in the cavity. Carefully increasing pump power and simultaneously slightly tuning the orientation of the polarization controllers, eventually a mode-locked pulse train with nearly identical pulse intensity as shown in Fig. 2(b) was obtained. The interval between the pulses is the same as that shown in Fig. 2(a). However, no pulse intensity modulation exists. Figure 2(d) shows the corresponding optical spectrum. It now has a clear discrete set of frequencies with the central four main spectral peaks having nearly identical strength, indicating that there is strong coupling among them. Comparing to the spectrum shown in Fig. 2(c), each spectral line shown in Fig. 2(d) also became narrower. We believe that it may be caused by the resonance between the MI frequency and the Lyot filter spectral spacing.

As the pump power was further increased, it was observed that a new pulse emerged on the side of each existing pulse. Carefully adjusting the pump strength and the orientation of the polarization controller, the two pulses always formed a bound state of solitons and the bound solitons as a unit have the repetition rate determined by the frequency spacing of the Lyot filter. Figures 3(a) and 3(b) show as an example two autocorrelation traces measured. In both cases the bound solitons have a repetition rate of 111.36 GHz, which is the same as that of the single-pulse train. Obviously the pulse separation in a bound state of solitons varied with the laser operation conditions. While the one shown in Fig. 3(a) has a pulse separation of ∼4.49 ps, the one shown in Fig. 3(b) has a pulse separation of ∼2.24 ps. The two bound solitons shown in Fig. 3(b) also have the same pulse intensity as can be identified from the measured autocorrelation trace. To our knowledge, the result shown in Fig. 3(b) is the first demonstration of an ultrahigh-repetition-rate bound-soliton pulse train.

We note that both the MI and the DFWM have played a role on the observed results. Different from the MIO laser whose pulse repetition rate increases with the pump power, the pulse repetition rate of our laser is fixed by the frequency spacing of the Lyot filter. However, different from the DFWM mode-locked fiber lasers, due to the influence of the strong MI multiple solitons are formed in our laser, which alters the repetition unit of the laser emission, e.g. in our experiment the laser can also emit the bound solitons. It is expected that with even stronger pumping, other multiple-pulse soliton train could also be obtained. However, it is to note that independent of the single-pulse or bound-soliton laser emission, the measured autocorrelation traces of the high-repetition pulses always exhibit a background. Similar results have also been observed in other ultrahigh-repetition-rate pulse lasers [1–4, 7, 9]. We point out that Schröder et

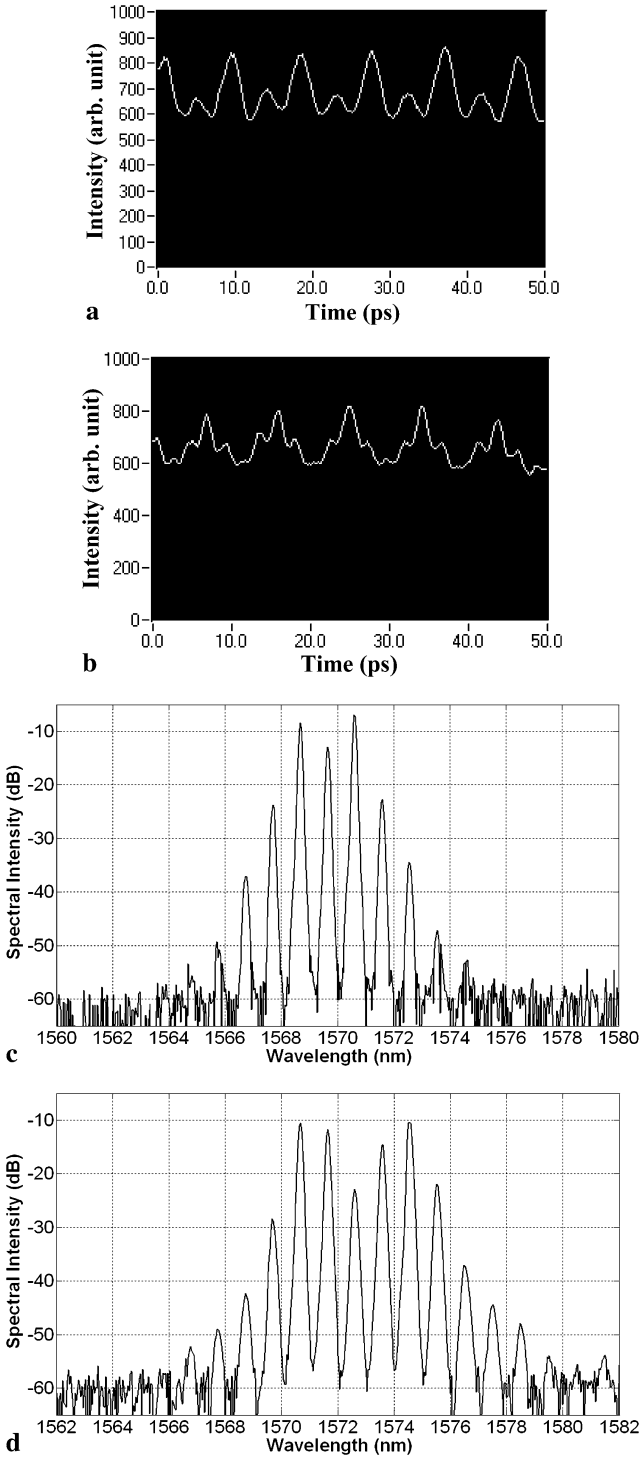

Fig. 3 Autocorrelation traces (**a**, **b**) and optical spectra (**c**, **d**) of the high-repetition-rate bound-soliton pulse emission of the fiber laser. From (**a**) to (**b**) the pump power was increased

al. have numerically studied the origin of the strong background on the autocorrelation traces of the passively mode-locked ultrahigh-repetition rate lasers [20]. They attributed it as caused by the supermode noise of the lasers. We believe that the strong background observed on the autocorrelation traces of our laser emission could also be traced back to the effect. In particular, in our laser the transmission lines of the Lyot filter could have a broader spectral width than those of a fiber Fabry-Pérot filter.

3 Numerical simulations

To give a better understanding on the formation of high-repetition-rate pulses in the fiber laser, especially the transition from the high repletion rate single soliton pulse train to the bound-soliton pulse train, we further conducted numerical simulations on the operation of the laser. The main difference of the current fiber laser to those of the passively mode-locked fiber lasers with the NPR technique is that it has a very large linear cavity birefringence. Consequently, the Lyot filter effect, which is an intrinsic feature of fiber lasers, becomes dominant in determining the operation of the laser. Self-started mode locking of the fiber laser is no longer caused by the NPR effect but by the DFWM process.

Therefore, we have used a model as described in [10] for our simulations. Briefly, we started the calculation with an arbitrary weak initial input and then circulated the light in the laser cavity. Whenever the pulse encountered an individual intracavity component, we multiplied the Jones matrix of the component to the light field to take account of the effect of the component. After one-roundtrip calculation, the output of the simulation was further used as the input of the next round of calculation. The calculation is continued until a steady state was established. For the simplicity of the numerical calculation we simplified the laser cavity as made of three parts: a waveplate, the various fiber segments, and a polarizer. The light propagation in the fibers was described by the coupled Ginzburg-Landau equations:

$$\begin{cases} \dfrac{\partial u}{\partial z} = -i\beta u + \delta\dfrac{\partial u}{\partial t} - \dfrac{ik''}{2}\dfrac{\partial^2 u}{\partial t^2} + \dfrac{ik'''}{6}\dfrac{\partial^3 u}{\partial t^3} \\ \qquad + i\gamma\left(|u|^2 + \dfrac{2}{3}|v|^2\right)u + \dfrac{i\gamma}{3}v^2u^* + \dfrac{g}{2}u \\ \qquad + \dfrac{g}{2\Omega_g^2}\dfrac{\partial^2 u}{\partial t^2} \\ \dfrac{\partial v}{\partial z} = i\beta v - \delta\dfrac{\partial v}{\partial t} - \dfrac{ik''}{2}\dfrac{\partial^2 v}{\partial t^2} + \dfrac{ik'''}{6}\dfrac{\partial^3 v}{\partial t^3} \\ \qquad + i\gamma\left(|v|^2 + \dfrac{2}{3}|u|^2\right)v + \dfrac{i\gamma}{3}u^2v^* + \dfrac{g}{2}v \\ \qquad + \dfrac{g}{2\Omega_g^2}\dfrac{\partial^2 v}{\partial t^2} \end{cases} \tag{2}$$

where u and v are the normalized envelopes of the optical pulses along the two orthogonal polarization axes of the fiber, u^* and v^* are the conjugate of u and v. $2\beta = 2\pi\,\Delta n/\lambda$

is the wave-number difference between the two polarization modes of the fiber, where Δn is the difference between the effective indices of the two modes, λ is the wavelength. $2\delta = 2\beta\lambda/2\pi c$ is the inverse group velocity difference, where c is the light speed. k'' is the second order dispersion coefficient, k''' is the third order dispersion coefficient and γ represents the nonlinearity of the fiber. g is the saturable gain coefficient of the fiber and Ω_g is the bandwidth of the laser gain. For undoped fibers $g = 0$, for the erbium-doped fiber, we further considered the gain saturation as:

$$g = G \exp\left[-\frac{\int (|u|^2 + |v|^2)\,\mathrm{d}t}{P_{\mathrm{sat}}}\right] \tag{3}$$

where G is the small signal gain coefficient and P_{sat} is the normalized saturation energy.

The following parameters were used to possibly match the experimental conditions and simultaneously keep the simulation as simple as possible: nonlinear fiber coefficient $\gamma = 3\ \mathrm{W}^{-1}\,\mathrm{km}^{-1}$, fiber dispersions $D''_{\mathrm{EDF}} = 10$ (ps/nm)/km, $D''_{\mathrm{SMF}} = 16$ (ps/nm)/km, and $D''' = 0.1$ (ps^2/nm)/km. The relationship between the dispersion parameter $D''$and the dispersion coefficient k'' is $D'' = -\frac{2\pi c}{\lambda^2}k''$. The cavity length is $L = 2.0_{\mathrm{SMF}} + 4.0_{\mathrm{EDF}} + 6.0_{\mathrm{SMF}} = 12$ m. The cavity birefringence was selected as 2×10^{-4} to match the ~125 GHz pulse repetition frequency. The gain saturation energy $P_{\mathrm{sat}} = 170$ pJ and the gain bandwidth was $\Omega_g = 12$ nm. In addition, a total cavity loss of 4 dB was introduced in the calculation.

Starting with an arbitrary weak initial pulse, numerically we found that a stable single-pulse train with the repetition rate of 125 GHz could always be obtained. A result is shown in Fig. 4(a). The result is clearly different from the case of fiber lasers with weak cavity birefringence, where, depending on the pumping strength, a single soliton or multiple solitons with undefined pulse separations will be obtained. The pulse separation (8 ps) in the cavity is determined by the FSR of the Lyot filter of the laser. Therefore, it confirms that the pulse train formation is due to the DFWM mode locking. We found that to obtain the stable ultrahigh-repetition-rate pulse train the small signal gain must be sufficiently strong. The result shown in Fig. 4(a) was obtained with a small signal gain of 29.3 dB/km. Starting from the state as shown in Fig. 4(a), when the small signal gain is increased to 34.3 dB/km, a stable ultrahigh-repetition-rate bound-soliton pulse train with exactly the same pulse repetition rate is obtained, as shown in Fig. 4(b). Figures 4(c) and 4(d) show the optical spectrum corresponding to Figs. 4(a) and 4(b), respectively. A clear spectral modulation corresponding to the pulse separation in the bound soliton can be identified in Fig. 4(d), which agrees with the experimental observation as shown in Fig. 3(d). Worth of mentioning is that like the experimentally measured spectrum of the high-repetition bound-soliton pulse train, the envelope of the calculated spectrum also exhibits a clear dip at their center, which is similar to the spectra of the bound states of solitons obtained in the NPR mode-locked fiber lasers [10]. In our numerical simulations as the pump strength is increased, the high-repetition-rate single soliton train was always first obtained, and then came the bound-soliton pulse train. No high-repetition-rate bound-soliton pulse train could be directly formed from an arbitrary initial pulse. As the high-repetition-rate bound-soliton pulse train was always formed from the high-repetition-rate single-pulse train after the pump is appropriately increased, it shows that it is also an intrinsic feature of the laser.

4 Discussion

Compare with other methods of achieving DFWM mode locking, e.g. introducing a spectral filter in the cavity [3, 4], our method is much simpler. Only a segment of HiBi fiber and an intracavity polarizer were inserted in the cavity, and when a polarization controller is also inserted in the cavity, tuning the orientation of the polarization controller the transmission peak positions of the Lyot filter can also be finely tuned. Moreover, the repetition rate of the generated pulse train can also be changed by changing the length of the HiBi fiber inserted.

Obviously, through increasing the frequency spacing of the Lyot filter an even higher-repetition-rate pulse train could be obtained in principle. Experimentally, we have shortened the length of the HiBi fiber to 1.3 m and further achieved a mode-locked pulse train with ~1 THz pulse repetition rate, as shown in Fig. 5. However, limited by the gain bandwidth of the erbium-doped fiber, no stable cw pulse train could be obtained. As 1 THz pulse train corresponds to 8 nm of the filter transmission peak spacing at 1550 nm, and the effective 3-dB gain bandwidth of the EDF is less than 20 nm, within our experimentally available pump strength it is difficult to generate the intracavity laser strength so that whose MI gain peak matches the filter FSR. Since the MI frequency is proportional to the square root of the average power in the cavity, a higher repetition rate needs much higher pump power.

5 Conclusions

In conclusion, we have firstly reported a high-repetition-rate bound-soliton fiber laser. We have shown experimentally that through inserting a segment of HiBi fiber together with a polarizer in a fiber ring laser, not only an ultrahigh-repetition-rate single-pulse soliton train, but also a bound-soliton pulse train can be formed in the laser. We have

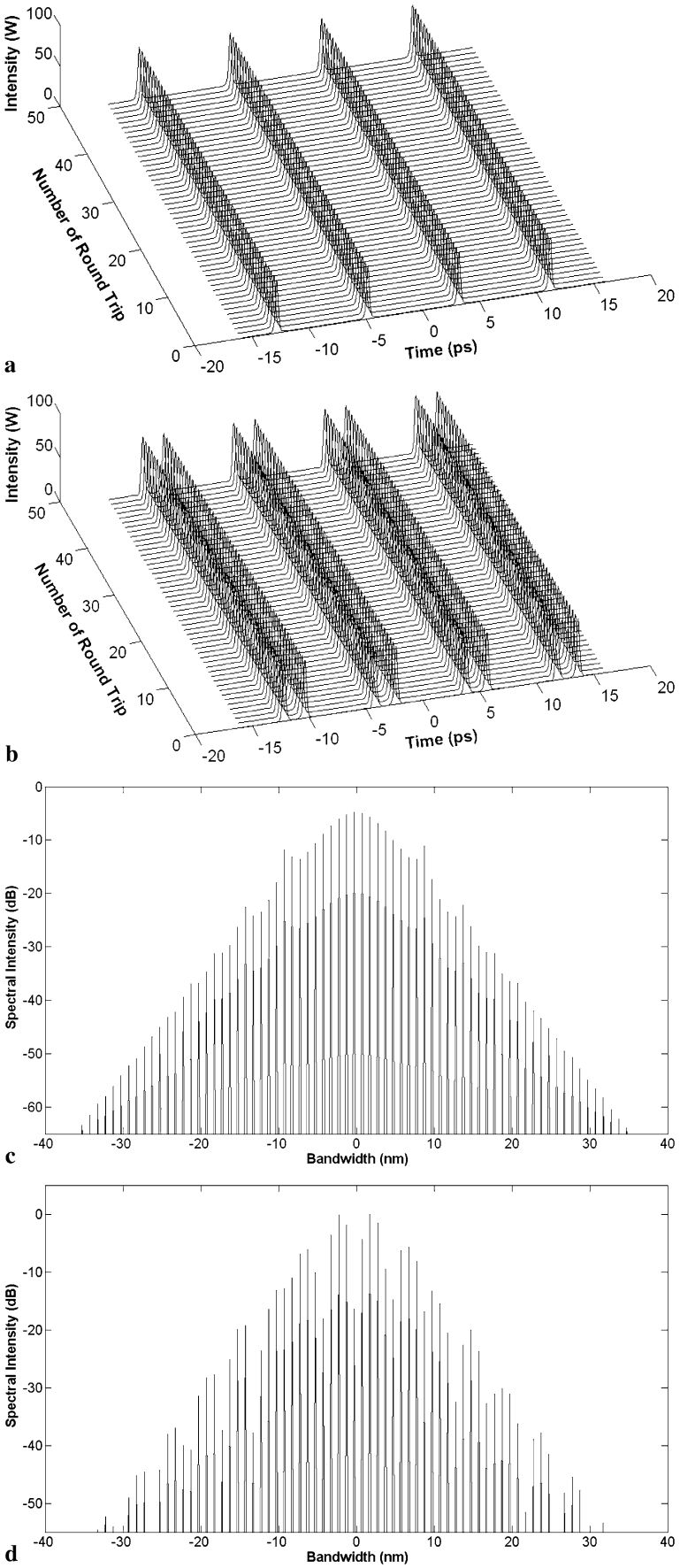

Fig. 4 Numerically simulated high-repetition-rate pulse emissions. (**a**) Single-pulse soliton train; (**b**) bound-soliton train; (**c**) optical spectrum corresponding to (**a**); (**d**) optical spectrum corresponding to (**b**)

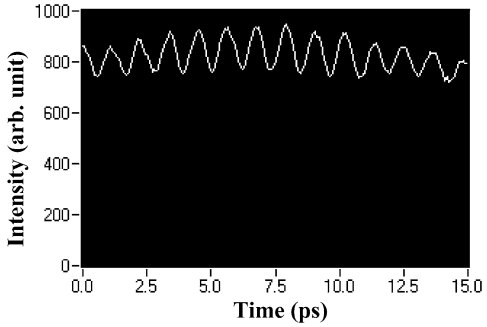

Fig. 5 Autocorrelation trace of a pulse laser emission with 1 THz pulse repetition rate

pointed out that the formation mechanism of the ultrahigh-repetition-rate bound-soliton pulses is due to the joint effect of the DFWM and the MI processes occurred in the laser. The experimental results are well reproduced by the numerical simulations. Furthermore, we note that an even higher-repetition-rate pulse train is in principle achievable in fiber lasers with broader gain bandwidth and higher pump power.

Acknowledgements L.M. Zhao acknowledges the Singapore Millennium Foundation for providing him a postdoctoral fellowship. This research was supported by the National Research Foundation Singapore under the contract NRF-G-CRP 2007-01.

References

1. P. Franco, F. Fontana, I. Cristiani, M. Midrio, M. Romagnoli, Opt. Lett. **20**, 2009 (1995)
2. C.J.S. de Matos, D.A. Chestnut, J.R. Taylor, Opt. Lett. **27**, 915 (2002)
3. E. Yoshida, M. Nakazawa, Opt. Lett. **22**, 1409 (1997)
4. P. Honzatko, P. Peterka, J. Kanka, Opt. Lett. **26**, 810 (2001)
5. A. Hasegawa, Opt. Lett. **9**, 288 (1984)
6. K. Tai, A. Hasegawa, A. Tomita, Phys. Rev. Lett. **56**, 135 (1986)
7. T. Sylvestre, S. Coen, P. Emplit, M. Haelterman, Opt. Lett. **27**, 482 (2002)
8. M. Quiroga-Teixeiro, C. Balslev Clausen, M.P. Sørensen, P.L. Christiansen, P.A. Andrekson, J. Opt. Soc. Am. B **15**, 1315 (1998)
9. J. Schroder, S. Coen, F. Vanholsbeeck, Opt. Lett. **31**, 3489 (2006)
10. D.Y. Tang, B. Zhao, D.Y. Shen, C. Lu, W.S. Man, H.Y. Tam, Phys. Rev. A **68**, 013816 (2003)
11. D.Y. Tang, L.M. Zhao, B. Zhao, Appl. Phys. B **80**, 239 (2005)
12. A.B. Grudinin, D.J. Richardson, D.N. Payne, Electron. Lett. **28**, 67 (1992)
13. B. Zhao, D.Y. Tang, P. Shum, Y.D. Gong, C. Lu, W.S. Man, H.Y. Tam, Appl. Phys. B **77**, 585 (2003)
14. A.B. Grudinin, D.J. Richardson, D.N. Payne, Electron. Lett. **29**, 1860 (1993)
15. B. Zhao, D.Y. Tang, P. Shum, W.S. Man, H.Y. Tam, Y.D. Gong, C. Lu, Opt. Commun. **229**, 363 (2004)
16. W.-W. Hsiang, C.-Y. Lin, Y. Lai, Opt. Lett. **31**, 1627 (2006)
17. L.N. Binh, N.D. Nguyen, T.L. Huynh, H.Q. Lam, In *Optical Fiber Communication Conference and Exposition and The National Fiber Optic Engineers Conference*, OSA Technical Digest (CD) (Optical Society of America, 2008), paper OThF4
18. L.M. Zhao, D.Y. Tang, F. Lin, B. Zhao, Opt. Express **12**, 4573 (2004)
19. L.M. Zhao, D.Y. Tang, B. Zhao, Opt. Commun. **252**, 167 (2005)
20. J. Schröder, D. Alasia, T. Sylvestre, S. Coen, J. Opt. Soc. Am. B **25**, 1178 (2008)